Journal of Organometallic Chemistry 896 (2019) 120–128

Contents lists available at ScienceDirect

Journal of Organometallic Chemistry

journal homepage: www.elsevier.com/locate/jorganchem

Evaluating stereoelectronic properties of bulky dialkylterphenyl phosphine ligands☆

Mario Marín [b], Juan J. Moreno [a, **], María M. Alcaide [a], Eleuterio Álvarez [a], Joaquín López-Serrano [a], Jesús Campos [a], M. Carmen Nicasio [b], Ernesto Carmona [a, *]

[a] Instituto de Investigaciones Químicas (IIQ), Departamento de Química Inorgánica and Centro de Innovación en Química Avanzada (ORFEO-CINQA), Consejo Superior de Investigaciones Científicas (CSIC) and Universidad de Sevilla, Avenida Américo Vespucio 49, 41092, Sevilla, Spain
[b] Departamento de Química Inorgánica, Universidad de Sevilla, Aptdo 1203, 41071, Sevilla, Spain

ARTICLE INFO

Article history:
Received 3 May 2019
Received in revised form
28 May 2019
Accepted 4 June 2019
Available online 7 June 2019

Keywords:
Bulky phosphine
Ligand parameterization
Tolman
Selenides
Buried volume
Terphenyl

ABSTRACT

The stereoelectronic properties of a series of sterically hindered phosphines containing a terphenyl substituent, PR_2Ar' (R = alkyl; Ar' = C_6H_3-2,6-Ar_2), have been evaluated by various methods. Their σ-donating capacity has been assessed on the basis of the carbon monoxide stretching frequencies in benchmark iridium [$IrCl(CO)_2(PR_2Ar')$] and rhodium [$Rh(acac)(CO)_2(PR_2Ar')$] (acac = acetylacetonate) complexes, as well as by measuring $^{31}P-^{77}Se$ scalar coupling constants ($^1J_{SeP}$) for the corresponding phosphine selenides ($Se=PR_2Ar'$). In turn, the steric profile of terphenyl phosphines has been gauged by calculating Tolman Cone Angle (TCA), ligand shielding (G) and percent buried volume (%V_{Bur}) parameters. These calculations have been carried out from both X-ray diffraction and DFT-optimized structures. We have also examined several of the widely used biaryl phosphines for comparative purposes.

1. Introduction

The stereoelectronic parameters associated with ancillary ligands play a crucial role in the control of the activity, selectivity and stability of transition metal catalysts [1]. In this regard, tertiary phosphines are key ligands in organometallic chemistry and homogeneous catalysis [2]. The facility with which their electronic and steric properties can be tuned in a precise manner, by changing the nature of the substituents attached to the P atom, has made of phosphines the most versatile ancillary ligands so far [3].

During the last two decades, several types of sterically demanding electron-rich phosphines have emerged as prominent supporting ligands in the context of C–C and C-heteroatom bond forming reactions [4]. Examples underlining this assertion include trialkyl phosphines like P^tBu_3 [1c,5] and heteroleptic phosphines [6] such as PAd_2R developed by Beller [7], ferrocenyl-derived phosphines introduced by Hartwig [8] and dialkylbiaryl phosphines put on stage by Buchwald [9]. The latter have become a large family of phosphines since their modular synthesis permits to customize the ligand for a particular application [10]. Currently, dialkylbiaryl phosphines are amongst the most effective ligands in Pd-catalyzed cross-coupling reactions [11].

Although the singular steric protection imparted by terphenyl fragments has been well documented [12], it is surprising that dialkylterphenyl phosphines, bearing a bulkier terphenyl group instead of the biaryl fragment, have been scarcely studied [13]. This motivated us a few years ago to investigate the synthesis and the coordination properties of this kind of ligands. First, we focused on the preparation of dialkylterphenyl phosphines PR_2Ar' (Ar' = terphenyl group) bearing methyl and ethyl substituents directly bound to the phosphorous atom and examined their coordination towards various late transition metals, namely Rh, Ir, Pt and Au [14]. These studies illustrated the ability of these phosphines to adopt different coordination modes, which not only involve the P atom but also weak M···C_{arene} interactions with one of the flanking aryl rings [13,14]. Later, the work was extended to the synthesis of branched and cyclic R-substituted PR_2Ar' phosphines. Regarding

☆ This paper is dedicated to the memory of Professor Pascual Royo, honoring his career and in recognition of his most valuable contribution to the development of Organometallic Chemistry in Spain.

* Corresponding author.
** Corresponding author.
E-mail address: guzman@us.es (E. Carmona).

https://doi.org/10.1016/j.jorganchem.2019.06.003
0022-328X/

ligand conformation, we concluded from these studies that dialkylterphenyl phosphines, PR_2Ar', may adopt one of three possible structures in the solid state, namely **A**, **B** and **C** in Fig. 1 [15], with the prevailing one resulting from the minimization of steric and electronic repulsions between the phosphine substituents and the phosphorus lone pair.

We also targeted the analysis of the σ-donor ability of our entire series of dialkylterphenyl phosphines by gathering IR data for Ni(0)–CO–phosphine compounds [15], $Ni(CO)_3(PR_2Ar')$, following Tolman's approach [16]. While the less sterically hindered phosphines (i.e. PMe_2Ar' and PEt_2Ar') formed the expected tricarbonyl adducts, those having the bulkier branched or cyclic alkyls groups, i.e. *i*Pr, *c*-C_5H_9 and *c*-C_6H_{11}, yielded uncommon dicarbonyl nickel complexes $Ni(CO)_2(PR_2Ar')$ instead, precluding a comparable estimation of their electronic features. A similar situation has been described for certain bulky ligands, such as biaryl phosphines and sterically demanding N-heterocyclic carbenes [17]. Among the alternative approaches developed to overcome this problem, the method introduced by Crabtree [18a], and later refined by Nolan [18b], consisting in measuring the C–O stretching frequencies for dicarbonyl iridium complexes $IrCl(CO)_2(L)$, is found to be the most general. Herein, we report on the preparation and characterization of a series of $IrCl(CO)_2(PR_2Ar')$ and $Rh(acac)(CO)(PR_2Ar')$ (where acac = acetylacetonate) compounds bearing the dialkylterphenyl phosphines outlined in Fig. 2. Their infrared carbonyl stretching frequencies have been measured to quantify the electronic parameter of PR_2Ar' ligands. These data have been compared with those obtained from measuring $^{31}P–^{77}Se$ scalar coupling constants ($^1J_{SeP}$) of phosphine selenides ($Se=PR_2Ar'$). To complement these studies, a thorough experimental and computational analysis of the steric parameters of this family of bulky phosphines has also been accomplished.

2. Results and discussion

2.1. Dialkylterphenyl phosphine iridium(I) and rhodium(I) carbonyl complexes

We previously reported the synthesis of iridium dicarbonyls $IrCl(CO)_2(PR_2Ar')$ with the PMe_2-containing phosphines **L9** and **L11** (Fig. 2) by a two-step procedure. First, $IrCl(COD)(PMe_2Ar')$ (COD = 1,5-cyclooctadiene) complexes were isolated from the reaction of the dimer $[IrCl(COD)]_2$ with ligands **L9** and **L11**, and then converted into the dicarbonyls by treatment with carbon monoxide in dichloromethane at room temperature [14c]. The same methodology was applied to the synthesis of the iridium derivatives with phosphines **L10** and **L12**. However, any attempts to isolate Ir-COD-phosphine adducts with sterically crowded ligands **L3**-**L8** resulted fruitless. Thus, the preparation of these iridium dicarbonyl complexes, **1·PR$_2$Ar'**, was accomplished in a one-pot synthesis, by reacting the corresponding phosphine with the Ir(I) dimer, in a 1:1 metal-to-ligand ratio, under an atmosphere of CO (Scheme 1). The reactions were carried out at 0 °C to avoid the formation of a recurrent, unidentified byproduct common to all examined phosphines, which diminished the yield of the expected dicarbonyl products. This method was also applied for the synthesis of complexes **1·L1** and **1·L2** based on the less bulky ligands **L1** and **L2**.

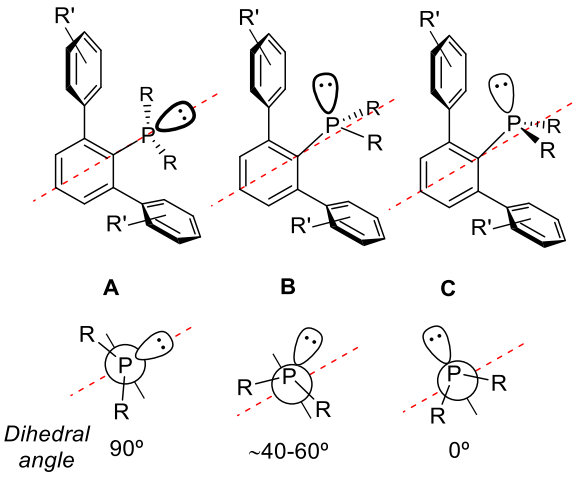

Fig. 1. Solid-state conformations for dialkylterphenyl phosphines.

Complexes bearing the phosphines **L1**, **L3**, **L6**, **L7**, **L10** and **L12** were isolated and spectroscopically characterized, but all others were only analysed by IR spectroscopy immediately after generation. Their $^{31}P\{^1H\}$ NMR resonances span a broad range, mainly depending on the nature of the R substituents, and appear shifted by *ca.* 15–33 ppm toward higher frequencies relative to the free phosphine ligands. This observation can be taken as suggestive of monodentate P-coordination of the terphenyl phosphine, void of $Ir\cdots C_{arene}$ interactions with a flanking aryl ring [15]. The ^1H NMR spectra of these species are in accordance with a symmetrical environment around the terphenyl moiety, most probably as a consequence of free rotation around the $P–C_{aryl}$ bond on the NMR time scale. Taking as an example compound **1·L1**, the four *t*Bu substituents on the side aryl rings give rise to only one resonance at 1.39 ppm and the two P–Me groups originate a doublet centred at 1.21 ppm ($^2J_{HP} = 9.8$ Hz). In the $^{13}C\{^1H\}$ NMR spectra of these dicarbonyl species, two different resonances are observed for the CO ligands, one at around 175–180 ppm ($^2J_{CP} \approx 115–125$ Hz) and the other at around 165–170 ppm ($^2J_{CP} \approx 11–13$ Hz), due to the CO molecule in *trans* and *cis* disposition to the phosphine ligand, respectively.

The molecular structures of **1·L1** and **1·L3** were confirmed by X-ray diffraction studies (Fig. 3). As expected, both compounds display a slightly distorted square-planar geometry. The phosphine ligand in complex **1·L1** adopts conformation **A** (Fig. 1), in which the two phosphine P–Me groups occupy the same region of space with reference to a plane containing the central aryl ring of the terphenyl moiety. In the perspective shown in Fig. 3, the two P–Me bonds are situated underneath this plane. Furthermore, the PMe_2 terminus is symmetrically arranged relative to the terphenyl central ring, inasmuch as the two $P\text{-}C_{ipso}\text{-}C_{ortho}$ angles are nearly identical at 120.5° and 121.0°. This conformation is alike that adopted by free PMe_2A^{Dtbp2}, **L1**, and generally, it is the preferred geometry for the least sterically demanding phosphines [15]. However, in the structures already described for **1·L9** and **1·L11**, the phosphine ligands exhibit the geometry defined as **B** in Fig. 1, where one of the P–Me bonds is almost coplanar with the terphenyl central ring, as a consequence of the increased steric demands brought about by the substituents at the 2 and 6 positions of the flanking rings [14c]. It is worth mentioning that, while in **1·L9** and **1·L11**, the planar $IrCl(CO)_2$ moiety is placed parallel to the neighbouring side ring, in **1·L1** one of the Ir–CO bonds (Ir1–C37) is nearly parallel to the $P–C_{ipso}$ bond ($C_{ipso}\text{-P-Ir-}C_{CO}$ torsion = −6.2(1)°). As a result, the $Ir(CO)_2Cl$ plane is approximately perpendicular to the central aryl ring.

Given that the free phosphine **L3** (Fig. 2), that contains branched isopropyl substituents and the terphenyl 2,6-C_6H_3-(3,5-C_6H_3-$(CMe_3)_2$), with 3,5-disubstituted lateral rings, adopts a structure of type **C** (Fig. 1), it might appear surprising that in the iridium complex **1·L3** (Fig. 3) the coordinated phosphine adopts the intermediate conformation **B**. In the latter arrangement, one of the P–C(H)Me_2 bonds almost eclipses the central aryl ring, that is, the said

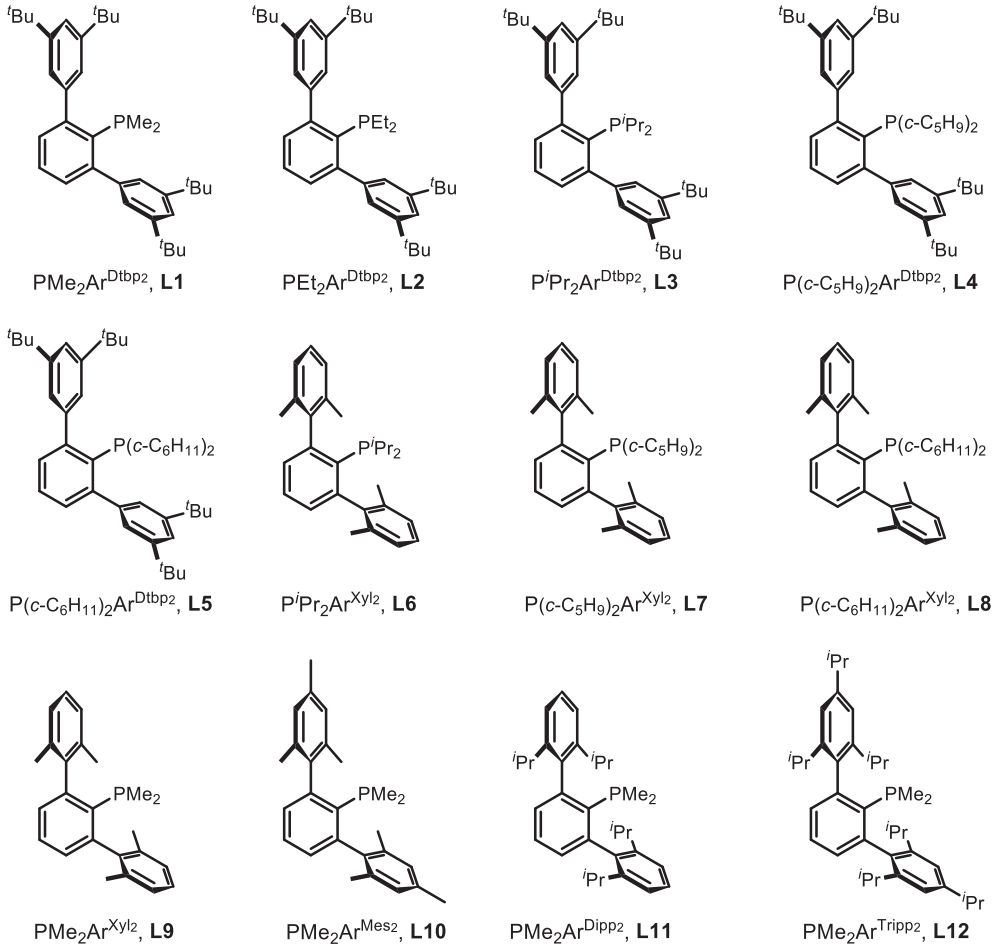

Fig. 2. Terphenyl phosphines used in this work.

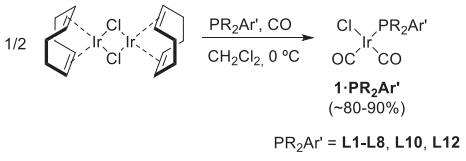

Scheme 1. Synthesis of $IrCl(CO)_2(PR_2Ar')$ complexes.

P–C(H)Me_2 bond and the two C_{ipso}-C_{ortho} bonds are practically coplanar. Despite somewhat stronger steric repulsions among the phosphine substituents in the **B** conformation in comparison with **C** [15], in the latter the phosphorus lone pair of electrons would point towards the proximal lateral ring, such that coordination to an $IrCl(CO)_2$ fragment, with no foreseeable readily dissociable ligands, would create unsustainable steric hindrance between the $IrCl(CO)_2$

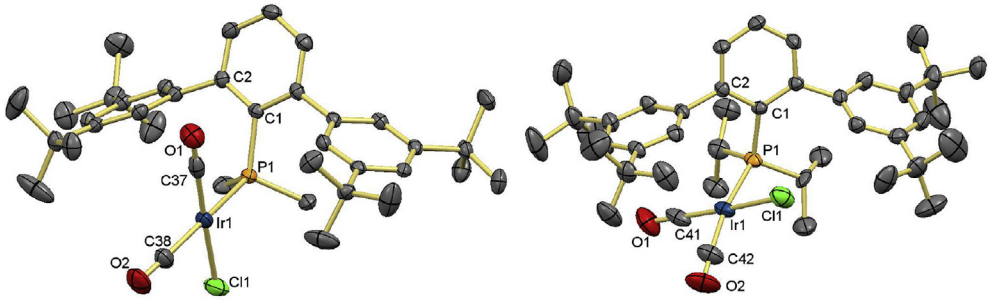

Fig. 3. Molecular structures of **1·L1** (left) and **1·L3** (right). Hydrogen atoms and minor disorder are omitted for clarity and thermal ellipsoids are set at 50% level probability. Selected bond distances (Å) and angles (°):**1·L1**: Ir1–P1 2.3599(6), Ir1–Cl1 2.3552(7), Ir1–C38 1.910(3), Ir1–C37 1.854(3), C37–O1 1.081(3), C38–O2 1.119(3), C37–Ir1–C38 92.85(12), C38–Ir1–Cl1 87.43(9), Cl1–Ir1–P1 87.48(2), P1–Ir1–C37 92.40(8), Ir1–P1–C1–C2 –87.50(17). **1·L3**: Ir1–P1 2.387(1), Ir1–Cl1 2.349(2), Ir1–C42 1.884(5), Ir1–C41 1.824(7), C41–O1 1.145(9), C42–O2 1.135(7), C41–Ir1–C42 90.5(3), C42–Ir1–Cl1 88.8(2), Cl1–Ir1–P1 87.33(5), P1–Ir1–C41 93.9(2), Ir–P1–C1–C2 –60.6(4).

moiety and the proximal 3,5-$C_6H_3(CMe_3)_2$ side ring. Hence, adoption of conformation **B** by the coordinated $P^iPr_2Ar^{Dtbp2}$ ligand in complex **1·L3**. Indeed, even under these premises, the iridium coordination plane deviates from planarity, with the CO ligand *trans* to phosphorus bending away from the neighbouring aromatic ring, forming a P1–Ir1–C42 bond angle of 170.1(2)°.

The C–O stretching frequencies recorded for complexes **1·PR$_2$Ar'** are collected in Table 1. As expected, due to the *cis* disposition of the CO ligands in these molecules, two ν_{CO} stretching bands were observed in their IR spectra. The TEP of the ligands can be determined from these values using the correlations developed by Crabtree [18a] and Nolan. [18b] The results of these calculations are shown in Table 1, which also includes, for comparison purposes, the TEP values of the less sterically hindered terphenyl phosphines determined from $Ni(CO)_3(PR_2Ar')$ [15] and those gathered for commercially available PMe_2Ph [18a] and the biaryl phosphine XPhos [17c]. It is clear that TEP values obtained from the $IrCl(CO)_2(L)$ complexes of terphenyl phosphines **L1**, **L2**, **L5**, **L9**-**L12**, as well as XPhos, differ from those observed for $Ni(CO)_3(L)$ by as much as 12 cm^{-1} (for **L1**). Furthermore, variation among the values for similar phosphines is relatively large (see, for example, the five dimethyl-substituted PMe_2Ar' phosphines, or dicyclohexyl-substituted **L5**, **L8** and XPhos). Thus, comparison of the IR data for different families of complexes should be made with caution.

For the sake of completeness, complexes $Rh(acac)(CO)(PR_2Ar')$, **2·PR$_2$Ar'** bearing the dialkyl terphenyl phosphines **L1**-**L12** and the biaryl phosphine XPhos, were also prepared following the synthetic pathway illustrated in Scheme 2. As above, a few representative examples, namely **2·L1**, **2·L2**, **2·L5** and **2·L7**, were isolated and spectroscopically characterized, whereas others were analysed solely by means of IR spectroscopy directly from the reaction mixture.

The $^{31}P\{^1H\}$ NMR spectra of these rhodium carbonyl compounds exhibit doublets ($^1J_{PRh}$ between 166 and 184 Hz) with δ values shifted *ca.* 54–68 ppm to higher frequency with respect to the uncoordinated phosphines. These Δδ values are significantly larger than those found for the iridium complexes discussed above, an observation for which no reasonable explanation can be given with data presently available. Likewise, their ^1H NMR spectra are fairly simple with only one set of resonances for the side aryl rings of the phosphine, consistent with a fast rotation of the phosphine in the NMR timescale at 25 °C. The carbonyl ligand resonance, which

Table 1
IR wavenumbers (cm^{-1}) for the C–O stretching vibrations in some $IrCl(CO)_2(L)$ complexes in CH_2Cl_2 solution.

Ligand	Complex	ν_{sym}	ν_{asym}	TEP (Ir)[a]	TEP (Ni)[b]
L1	$IrCl(CO)_2(PMe_2Ar^{Dtbp2})$	2063	1984	2051.1	2063
L2	$IrCl(CO)_2(PEt_2Ar^{Dtbp2})$	2061	1983	2049.8	2061
L3	$IrCl(CO)_2(P^iPr_2Ar^{Dtbp2})$	2060	1980	2048.2	–
L4	$IrCl(CO)_2(PCyp_2Ar^{Dtbp2})$	2058	1978	2046.5	–
L5	$IrCl(CO)_2(PCy_2Ar^{Dtbp2})$	2056	1980	2046.5	2060
L6	$IrCl(CO)_2(P^iPr_2Ar^{Xyl2})$	2064	1982	2050.7	–
L7	$IrCl(CO)_2(PCyp_2Ar^{Xyl2})$	2063	1979	2049.0	–
L8	$IrCl(CO)_2(PCy_2Ar^{Xyl2})$	2062	1980	2049.0	–
L9	$IrCl(CO)_2(PMe_2Ar^{Xyl2})$	2068	1987	2054.5	2063.8
L10	$IrCl(CO)_2(PMe_2Ar^{Mes2})$	2066	1986	2053.2	2063
L11	$IrCl(CO)_2(PMe_2Ar^{Dipp2})$	2067	1987	2054.1	2062.9
L12	$IrCl(CO)_2(PMe_2Ar^{Tripp2})$	2065	1986	2052.8	2062
XPhos	$IrCl(CO)_2(PCy_2Ar^{Tripp})$[c]	2070	1985	2053.3	2059
PMe_2Ph	$IrCl(CO)_2(PMe_2Ph)$[d]	2084	1999	2066.4	2065.3[e]

[a] Calculated using the correlation found in ref. [18].
[b] From ref. [15].
[c] From ref. [17c].
[d] From ref. [18].
[e] From ref. [16a].

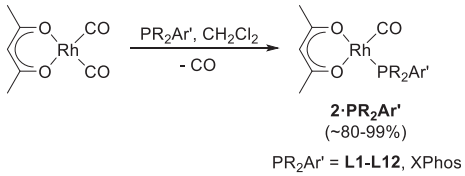

Scheme 2. Synthesis of $Rh(acac)(CO)(PR_2Ar')$ complexes.

appears at a chemical shift of around 190–192 ppm in the $^{13}C\{^1H\}$ NMR spectra, also shows the coupling with the two magnetically active nuclei ($^1J_{CRh} \approx 77$ Hz, $^2J_{CP} \approx 24$ Hz).

In the solid state structure (Fig. 4), the molecules of **2·L1** show a disposition similar to the iridium analogue **1·L1**, that is, with the phosphine adopting conformation of type **A** and the Rh(acac)(CO) fragment contained in the symmetry plane perpendicular to the central aryl ring of the terphenyl moiety.

Finally, C–O stretching frequencies recorded for these complexes span the range 1954–1963 cm^{-1} (see Supplementary Data, Table S1). As in the case of the iridium complexes discussed above, IR data do not correlate well with the TEPs observed in the $Ni(CO)_3(L)$ complexes [15]. However, there is a moderately good correlation (Fig. S1) between the ν_{CO} values in $IrCl(CO)_2(L)$ and $Rh(acac)(CO)(L)$ complexes of the phosphines described here. This permits using either of the metal-phosphine systems studied, namely $IrCl(CO)_2(PR_2Ar')$ or $Rh(acac)(CO)(PR_2Ar')$, to compare the donor capacity of the terphenyl phosphine ligands.

2.2. Dialkylterphenyl phosphine selenides

To complete our studies on the evaluation of the σ-donor capacity of dialkylterphenyl phosphines we prepared their corresponding selenides $Se{=}PR_2Ar'$ and examined the resulting one-bond $^{31}P–^{77}Se$ scalar coupling constants ($^1J_{PSe}$) [19]. In related studies, the distinctive chemical shifts of selenoureas (^{77}Se) and phosphinidenes (^{31}P) have also been used to estimate the π-accepting character of N-heterocyclic carbenes [20], although this lies out of the scope of the present work. Selenides $Se{=}PMe_2Ar^{Dtbp2}$ and $Se{=}P^iPr_2Ar^{Xyl2}$ were isolated and fully characterized, and their molecular structures elucidated by X-ray crystallography, while for all other phosphines studied, corresponding selenides were generated in solution and the $^1J_{PSe}$ coupling constant determined.

As expected, the solid-state structures of selenides $Se{=}PMe_2Ar^{Dtbp2}$ and $Se{=}P^iPr_2Ar^{Xyl2}$ (Fig. 5) are alike those of the

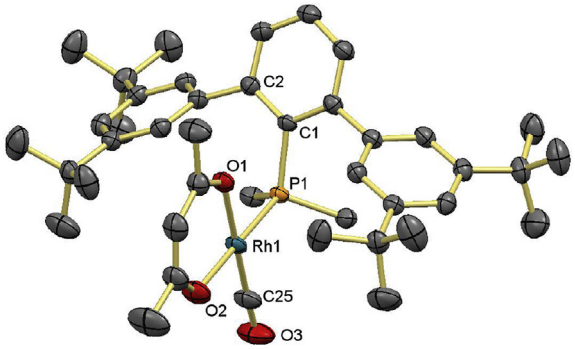

Fig. 4. Molecular structure of $Rh(acac)(CO)(PMe_2Ar^{Dtbp2})$, **2·L1**. Hydrogen atoms and minor disorder are omitted for clarity and thermal ellipsoids are set at 50% level probability. Selected bond distances (Å) and angles (°): Rh1–P1 2.2374(11), Rh1–O1 2.051(3), Rh1–O2 2.068(3), Rh1–C25 1.797(5), C25–O3 1.162(7), P1–Rh1–O1 92.22(9), O1–Rh1–O2 88.65(14), O2–Rh1–C25 91.90(19), C25–Rh1–P1 87.23(16), Rh1–P1–C1–C2 −94.0(3).

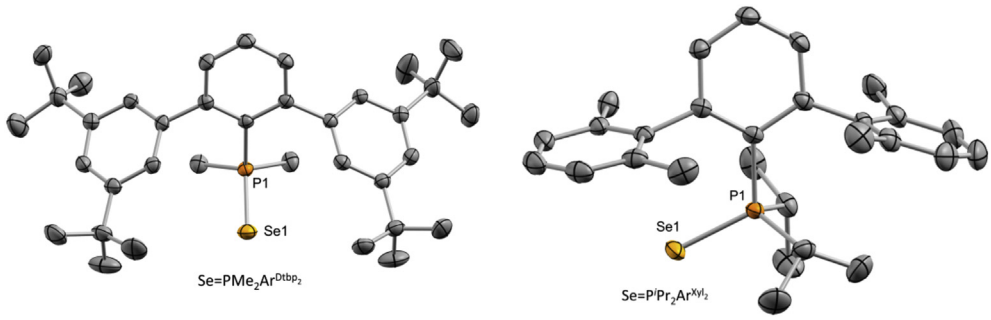

Fig. 5. Molecular structure of compounds Se=PMe_2Ar^{Dtbp2} and Se=$P^iPr_2Ar^{Xyl2}$, hydrogen atoms have been excluded for clarity and thermal ellipsoids are set at 50% probability.

free phosphines, namely **A** and **C**, respectively, thus retaining the favoured conformation. It is therefore evident that selenium binding to phosphorus does not alter significantly the steric hindrance in the proximity of the phosphorus atom in these structures. For Se=PMe_2Ar^{Dtbp2}, the C_{ipso}-P-Se plane is almost perpendicular to the central ring, with a dihedral angle of 92.1°. In the $P^iPr_2Ar^{Xyl2}$ derivative, though, the above-mentioned two planes are practically coincident and the dihedral angle is of only 0.6°. For the two compounds the P–Se distance is close to 2.12 Å, and for Se=$P^iPr_2Ar^{Xyl2}$ the separation of the Se atom from the centroid of the neighbouring Xyl ring is of 3.6 Å. This distance is practically identical to the sum of the van der Waals radii of selenium and carbon (3.59 Å) [21], hinting at the existence of weak dispersion forces [22] that may contribute to stabilize additionally the observed structure. The angular symmetric deformation coordinate, *S4'*, defined by Orpen [23] as the sum of the Se–P–C angles minus the sum of the C–P–C angles, is larger in Se=PMe_2Ar^{Dtbp2} than in Se=$P^iPr_2Ar^{Xyl2}$ (22.7 *vs.* 15.4°), thereby indicating a smaller cone angle for the former compared to the latter. A more detailed analysis of the steric factors will be described in the next section.

As mentioned briefly, the magnitude of $^1J_{PSe}$ was determined for all terphenyl phosphines investigated. To reduce solvent effects [24] on scalar coupling constant values, we carried out NMR-tube experiments in C_6D_6 as a non-polar solvent. The results of these measurements are collected in Table 2. It is pertinent to recall that $^1J_{PSe}$ is sensitive to the hybridization of the P atom, specifically to the atomic *s*-character of the lone-pair of electrons [25]. According to Bent's rule, *s*-character tends to concentrate in orbitals bonding to the more electropositive substituents [26]. Hence, Se=PR_3 derivatives of scarcely donating phosphines present larger $^1J_{PSe}$ couplings than analogues of electron-rich phosphines, as illustrated by the 732 and 684 Hz values determined for PPh_3 and PMe_3, respectively, in CD_2Cl_2 [27]. It must be remarked, however, that steric hindrance can also play a role and may even contribute to $^1J_{PSe}$ opposing electronic effects [28]. This phenomenon is probably responsible for the $^{31}P–^{77}Se$ couplings of 693, 692 and 684 Hz gauged for P^iPr_3, P^tBu_3 and PMe_3 (CD_2Cl_2), in disagreement with the trend expected from tabulated Tolman electronic parameters of 2059.2 (P^iPr_3), 2056.1 (P^tBu_3) and 2064.1 cm^{-1} (PMe_3) [3].

Table 2
$^1J_{SeP}$ coupling constants (Hz, C_6D_6) of terphenyl phosphine selenides (Se=PR_2Ar').

Ligand	$^1J_{SeP}$
L1, PMe_2Ar^{Dtbp2}	710
L2, PEt_2Ar^{Dtbp2}	708
L3, $P^iPr_2Ar^{Dtbp2}$	710
L4, $P(c\text{-}C_5H_9)_2Ar^{Dtbp2}$	754
L5, $P(c\text{-}C_6H_{11})_2Ar^{Dtbp2}$	747
L6, $P^iPr_2Ar^{Xyl2}$	751
L7, $PCyp_2Ar^{Xyl2}$	751
L8, PCy_2Ar^{Xyl2}	747
L9, PMe_2Ar^{Xyl2}	709[a]
L10, PMe_2Ar^{Mes2}	708[a]
L11, PMe_2Ar^{Dipp2}	704[a]
L12, PMe_2Ar^{Tripp2}	703[a]
PMe_3	712
$P(c\text{-}C_5H_9)_3$	714

[a] Fom ref.[14c].

Notwithstanding these shortcomings, some comments on the $^1J_{PSe}$ coupling constants collected in Table 2 are appropriate. In close analogy with previously studied PMe_2Ar' phosphines [14c], PMe_2Ar^{Dtbp2} has a $^{31}P–^{77}Se$ coupling of 710 Hz, also very close to the value determined in parallel C_6D_6 experiments for PMe_3 (712 Hz). No relevant variations were encountered for PEt_2Ar^{Dtbp2}, (**L2**) or $P^iPr_2Ar^{Dtbp2}$ (**L3**), although the analogous cyclopentyl and cyclohexyl phosphines, **L4** and **L5**, yield significantly higher coupling constants of 754 Hz and 747 Hz for **L4** and **L5**, respectively, possibly due to the contribution of steric effects. These data contrast with their corresponding TEP calculated from iridium carbonyl compounds of type $IrCl(CO)_2(PR_2Ar')$, for which the latter phosphines revealed themselves as better overall σ-donors (see Table 1). It is nevertheless of note that for PMe_2Ar^{Dtbp2} and $P(c\text{-}C_5H_9)_2Ar^{Dtbp2}$ the sum of the C–P–C angles increases from 298.5 to 309°. Similarly, $P^iPr_2Ar^{Xyl2}$ (**L6**), $P(c\text{-}C_5H_9)_2Ar^{Xyl2}$ (**L7**) and $P(c\text{-}C_6H_{11})_2Ar^{Xyl2}$ (**L8**), with wider C–P–C bond angles summing 315.9, 313.9 and 316.6°, respectively, exhibit unexpectedly high $^1J_{PSe}$ coupling constants of 751, 751 and 747 Hz. For comparative purposes, we also determined in C_6D_6 a coupling constant of 714 Hz for $P(c\text{-}C_5H_9)_3$. Within the PMe_2Ar' series, the values of $^1J_{PSe}$ correlate better with the trend expected on the basis of the electron-donation ability of the terphenyl substituents. Thus, the σ-donor capacity follows the order $PMe_2Ar^{Tripp2} > PMe_2Ar^{Dipp2} > PMe_2Ar^{Mes2} > PMe_2Ar^{Xyl2}$.

Taken together, these results suggest that the use of $^{31}P–^{77}Se$ scalar coupling constants as a method to evaluate the σ-donor capacity of phosphines may be appropriate for series of ligands with comparable front strain, as it occurs with the PMe_2Ar' series (**L9-L12**). The approach may, however, fail when phosphines with dissimilar steric profiles are collated. Correlations of this kind are particularly valuable for ligand screening in catalytic applications, where subtle modifications on the electronics around the metal centre (with steric factors virtually unaltered) may have important effects in catalytic performance (i.e. CH_3 substitution by CF_3 at a remote position from the metal). On the contrary, results derived from CO stretching frequencies in Ir and Rh complexes for the same PMe_2Ar' series do not correlate with the expected electron-donating capacity of the terphenyl moiety, as revealed by the following trends in the values of TEP. For iridium, $PMe_2Ar^{Tripp2} > PMe_2Ar^{Mes2} > PMe_2Ar^{Dipp2} > PMe_2Ar^{Xyl2}$ (Table 1); whereas for rhodium, $PMe_2Ar^{Tripp2} = PMe_2Ar^{Mes2} = PMe_2Ar^{Xyl2} > PMe_2Ar^{Dipp2}$ (Table S1)). In these square-planar complexes, the

CO stretching frequencies appear not to be sensitive to front strain interactions. Thus, as shown in Tables 1 and S1, increasing the electron-donating ability of the R groups in PR_2Ar' series invariably leads to reduced ν_{CO} values, thus differing from the conclusions that could be extracted from $^1J_{PSe}$ coupling constants analysis. Considering the above, it is clear that the use of either CO stretching frequencies in nickel, iridium or rhodium carbonyl compounds, or $^{31}P-^{77}Se$ scalar coupling constants, to grade ligand σ-donation should be done with caution. It is also evident that a combination of the different available methods provides the most reliable conclusions.

2.3. Steric properties of dialkylterphenyl phosphines

Among the available parameters utilized to gauge ligand steric properties, the Tolman Cone Angle (TCA) emerged in the 1970s as a key tool to provide a simple and effective model to rationalize the sterics of phosphine ligands [3]. Mingos' posterior contribution [29] permitted the use of crystallographic data (cTCA) instead of CPK models. $Ni(CO)_3(PR_3)$ complexes were first proposed as benchmark species to parameterize stereoelectronic properties of phosphine ligands. However, additional carbonyl loss takes place when polydentate or very bulky phosphines are employed, discarding these species as proper candidates for a general assessment of crystallographic TCAs. As an alternative, the molecular geometry of $AuCl(PR_3)$ complexes has been extensively determined for the above purposes. However, for dialkylbiaryl and -terphenyl phosphines, a lateral aryl ring from the ligand is in almost every case placed near the gold atom [14b,30], and therefore a pseudo bidentate P-plus-C_{arene} coordination mode is formally achieved, leading to exceedingly high values of measured cone angles. On this basis, we decided to analyse some individual descriptors of steric properties for the dialkylterphenyl phosphines **L1-L12** in their $IrCl(CO)_2(PR_2Ar')$ complexes (**1·Ln**), which have been obtained from experimental solid state X-Ray data and from calculated geometries.

This section focuses on results from Tolman Cone Angle (TCA) [3,28], ligand shielding G [31], and % Buried Volume ($\%V_{Bur}$) [32] calculations. The latter yields the percentage of the volume of a sphere centred on the metal with a given radius (3.5 Å) which is occupied by the ligand, and describes very appropriately steric hindrance in the first coordination sphere of the metal whereas the cone angle is sensitive to ligand size at a distance [33]. The ligand shielding parameter G, or percentage of the metal M coordination sphere shielded by a given ligand, and its equivalent cone angle, ECA (θ), as implemented in the Solid-G program [34], have been used recently to calculate equivalent cone angles of phosphines to rationalize the yields of Suzuki reactions [35] and to calculate steric effects of simplified surrogate ligands in amine arylation catalysis, finding a direct correlation between G and $\%V_{Bur}$ [36].

Table 3 summarizes structural data from calculated (see the supporting information for details) and experimental (from X-ray diffraction analysis; denoted with an asterisk) molecular structures of complexes $IrCl(CO)_2(PR_2Ar')$, **1·Ln**. Values of angular symmetric deformation coordinate S4' [20] have been included for comparison with those reported previously for some of these phosphines in $Ni(CO)_3(PR_2Ar')$ and $Ni(CO)_2(PR_2Ar')$ complexes [15]. Interestingly, there is no correlation between the values reported here and those found for the nickel complexes. Besides, it is difficult to compare the steric demands of **L1-L12** with those of biaryl phosphines collected in entries 13–17 [37], which may be a reflection of the flexibility of terphenyl phosphine ligands.

However, analysis of $\%V_{Bur}$ and cone angles (see Figs. 6 and 7) reveals different steric regimes for the studied phosphines. While it is difficult to interpret all features in the cited Table 3 and Figs. 6 and 7, some trends arise from the represented data. First, the conspicuous difference between the calculated and experimental $\%V_{Bur}$ values for **Ir·L1** may be attributed to the incapacity of the dispersion-corrected DFT method used to reproduce its experimental molecular geometry, or to crystal packing effects that may compress significantly the phosphine ligand in the solid state structure. Interestingly, the difference becomes smaller in the cone angle values, which ascribed reduced steric bulk to **L5**, bearing two cyclohexyl groups attached to phosphorous, than to the rest of the $PR_2(C_6H_4\text{-}3,5\text{-}t\text{Bu}_2)$ series. While the origin of this is not obvious, it is worth mentioning that the optimized geometries for **Ir·L4** and **Ir·L5** reveal different phosphine conformations, of types **C** and **A**, respectively (Fig. 1). The different orientation of the PR_2 fragment relative to the central aryl ring in conformations **A** and **C** would naturally give rise to different steric strains in the two systems. This trend is also reflected, albeit to a lesser extent, in the cone angles of the phosphine-oxide and -selenide surrogates, whose corresponding steric descriptors have also been obtained (see Table S2 in the Supporting Information).

Leaving aside individual metrics, the present $\%V_{Bur}$ calculations allow distinguishing three types of ligands, namely the Buchwald-

Table 3
Selected structural parameters for complexes of type $IrCl(CO)_2(PR_2Ar')$ (**1·PR$_2$Ar'**).

Complex	S4′(°)	TCA (°) (2.28)	$\%V_{bur}$ (2.28)	ECA (°) (2.28)	G 2.28(%)
1·L1	*26.9	152.35/*149.6	41.6/*35.5	170.4/*158.6	45.8/*40.7
1·L2	23.7	172.6	49.9	172.97	46.93
1·L3	8.7	196.8/*193.9	45.2/*43.4	179.3/180.0	49.7/50.0
1·L4	25.7	212.4	46.7	187.29	53.18
1·L5	14.8	177.4	45.5	180.51	50.22
1·L6	*10.8	186.5/*183.4	45.3/*45.6	172.01/*170.2	46.5/*45.71
1·L7	6.8	187.1	45.4	171.82	46.43
1·L8	13.2	187.3	45.2	173.34	47.09
1·L9[a]	*16.2	153.9/*148.7	38.6/*38.6	154.2/*152.04	38.8/*37.9
1·L10	15.9	153.7	38.9	157.12	40.08
1·L11[a]	*13.9	159.8/*159.1	39.8/*39.3	165.5/*158.9	43.7/*40.9
1·L12	20.2	169.9	41.1	174.08	47.42
1·PCy2Ph[b]	*20.0	*143.7	*30.8	*134.3	*30.6
1·(Cy-JohnPhos)[b]	*11.0	*157.5	*34.2	*142.1	*33.8
1·(Me-Phos)[b]	*4.5	*158.5	*34.7	*143.4	*34.3
1·(S-Phos)[b]	*12.2	*153.5	*32.8	*141.8	*33.6

*From X-ray data; Cy-JohnPhos = $PCy_2(C_6H_4\text{-}2\text{-}Ph)$; Me-Phos = $PCy_2(C_6H_4\text{-}2\text{-}(C_6H_4\text{-}2'\text{-}CH_3))$; S-Phos = $PCy_2(C_6H_4\text{-}2\text{-}(C_6H_3\text{-}2',6'\text{-}(OMe)_2))$; X-Phos = $PCy_2(C_6H_4\text{-}2\text{-}(C_6H_2\text{-}2',4',6'\text{-}{}^i\text{Pr}_3))$.

[a] Recalculated from ref [14c].

[b] Recalculated from ref [34].

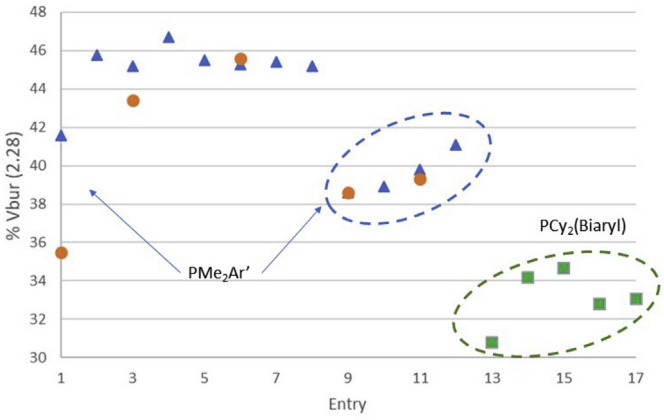

Figure 6. % Buried Volume for dialkylterphenyl and dicyclohexylbiaryl phosphines in **1·Ln** complexes. Blue triangles denote values calculated from DFT-optimized geometries, orange circles and green squares are for values obtained from crystallographic data of dialkylterphenyl phosphine and dialkylbiaryl phosphine complexes, respectively.

type dicyclohexylbiaryl phosphines, dimethylterphenyl phosphines **L1** and **L9-L12**, and other terphenyl phosphines with bulkier R groups directly bound to the phosphorous atom (Fig. 6). In addition, Tolman Cone Angle (TCA) data, which are known to reflect the effect of substituents on the ligand that are beyond the first coordination sphere of the metal, extend this classification to four groups, with the larger cone angle values corresponding to phosphines with C_6H_3-3,5-*t*Bu_2 aryl rings on their terphenyl moiety, followed by P^iPr_2 and PMe_2 terphenyl phosphines and finally, PCy_2(Biaryl) with the smaller values (Fig. S4).

Taking into account crystallographic data only, Fig. 7 reveals that the terphenyl phosphines discussed in this work appear to exert their steric bulk closer to the metal center in their square planar $IrCl(CO)_2$ L complexes than their PCy_2(Biaryl) counterparts. This is suggested by the better correlation of the TCAs with larger $\%V_{Bur}$ found for the former in comparison with the biaryl phosphines of comparable TCAs. This may be in part due to the presence of smaller R substituents at the phosphorous atom of the terphenyl phosphines relative to the bulky cyclohexyl groups of their biaryl counterparts [38].

3. Experimental section

3.1. General considerations

All preparations and manipulations were carried out under an atmosphere of dry oxygen-free dinitrogen by means of standard Schlenk or glovebox techniques. Solvents were rigorously dried and degassed before use. Ar'MgBr were prepared by following the synthesis reported by Power [39] for the related Ar^{Xyl2} compounds without adding I_2 in the last step of the preparation. Ligands **L1**-**L12** [14c,15] and complexes $Ni(cod)_2$ [40] and $[Ir(cod)]_2(\mu\text{-}Cl)_2$ [41] were synthesized by following previously reported procedures. PCl_3 was distilled prior to use and kept under a nitrogen atmosphere. Other chemicals were purchased from commercial sources and used as received. Solution NMR spectra were recorded on Bruker Avance DPX-300, DRX-400 and DRX-500, and 400 Ascend/R spectrometers. The ^1H and ^{13}C resonances of the solvent were used as the internal standard and the chemical shifts are reported relative to TMS while ^{31}P was referenced to external H_3PO_4. Infrared spectra were recorded on a Bruker Vector 22 Microanalyses were performed by the Microanalytical Service of the Instituto de Investigaciones Químicas (IIQ). X-ray diffraction data were collected on Bruker Nonius X8 APEX-II. CCDC 1912865 (**1-L1**), 1912866 (**2-L3**), 1912867 (**2-L1**) 1912868 (Se=PMe_2Ar^{Dtbp2}) and 1912869 (Se=$PiPr_2Ar^{Xyl2}$) contain the supplementary crystallographic data for this paper. These data can be obtained free of charge from The Cambridge Crystallographic Data Centre.

3.2. Synthesis of representative metal complexes

IrCl(CO)$_2$(PMe$_2$Ar^{Dtbp2}), 1·L1. CH_2Cl_2 (3 mL) was added to a Schlenk tube charged with $[Ir(\mu\text{-}Cl)(cod)]_2$ (0.0337, 0.050 mmol) and PMe_2Ar^{Dtbp2} (0.0570 g, 0.105 mmol, 5% excess). After stirring for 30 min, the vessel was cooled to 0 °C and charged with CO

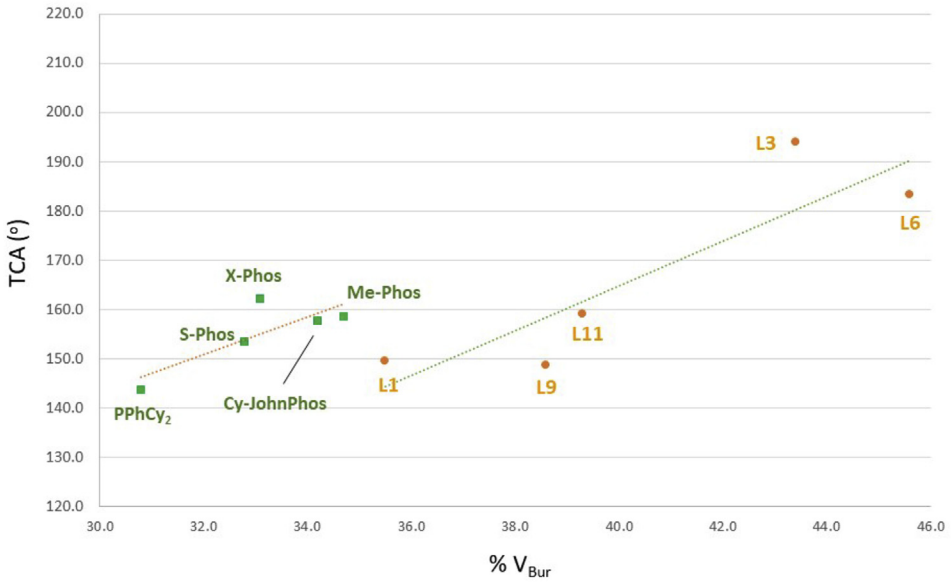

Fig. 7. Tolman Cone Angle (°) vs $\%V_{Bur}$ for dialkylterphenyl and dialkylbiaryl phosphines in 1·Ln complexes. Orange circles and green squares are for values obtained from crystallographic data of dialkylterphenyl phosphine and dialkylbiaryl phosphine complexes, respectively. (For interpretation of the references to color in this figure legend, the reader is referred to the Web version of this article.)

(0.9 bar). After the cool bath was removed, the solution was left to evolve from the initial red into yellow (*ca.* 1 h). The volatiles were evaporated under vacuum and the resulting residue was washed with pentane at −30 °C, rendering an intensely colored yellow solid. Yield: 0.0677 g, 85%. Samples suitable for X-ray diffraction were obtained by slow evaporation from a pentane solution at room temperature. IR (CH_2Cl_2): $\nu_{CO} = 2063, 1984\ cm^{-1}$. Anal. Calcd. for $C_{38}H_{51}ClIrO_2P$: C, 57.16; H, 6.44. Found: C, 56.81; H, 6.84. ^1H NMR (300 MHz, C_6D_6, 298 K): δ 7.59 (t, $^4J_{HH} = 1.8$ Hz, 2 H, *p*-Dtbp), 7.54 (d, $^4J_{HH} = 1.8$ Hz, 4 H, *o*-Dtbp), *ca.* 7.16 (*m*-C_6H_3), 7.04–6.99 (m, 1 H, *p*-C_6H_3), 1.39 (s, 36 H, CH_3 ^{t}Bu), 1.21 (d, $^2J_{HP} = 9.8$ Hz, 6 H, CH_3 Me). $^{13}C\{^1H\}$ NMR (100 MHz, C_6D_6, 298 K): δ 179.1 (d, $^2J_{CP} = 126$ Hz, *CO trans* P), 170.2 (d, $^2J_{CP} = 13$ Hz, *CO cis* P), 151.2 (s, *m*-Dtbp), 149.20 (d, $^2J_{CP} = 9$ Hz, *o*-C_6H_3), 142.28 (d, $^3J_{CP} = 4$ Hz, *ipso*-Dtbp), 131.4 (d, $^3J_{CP} = 8$ Hz, *m*-C_6H_3), 130.0 (d, $^4J_{CP} = 2$ Hz, *p*-C_6H_3), *ca.* 129 (*ipso*-C_6H_3), 125.3 (s, *o*-Dtbp), 122.4 (s, *p*-Dtbp), 35.2 (s, $C(CH_3)_3$ ^{t}Bu), 31.7 (s, CH_3 ^{t}Bu), 17.13 (d, $^2J_{CP} = 38$ Hz, CH_3 Me). $^{31}P\{^1H\}$ NMR (202 MHz, C_6D_6, 298 K): δ −3.5.

Rh(acac)(CO)(PMe$_2$Ar^{Dtbp2}), 2·L1. THF (2 mL) was added to a Schlenk tube charged with $Rh(acac)(CO)_2$ (0.0129 g, 0.050 mmol) and PMe_2Ar^{Dtbp2} (0.0271 g, 0.053 mmol). The mixture was stirred for 90 min and then taken to dryness. The resulting residue was washed with pentane, extracted in CH_2Cl_2 and filtered to a weighed vial. Removal of volatiles, first under a N_2 flow and then under vacuum, rendered the sought product as a yellow solid. Yield: 0.0297 g, 80%. The samples thus obtained are suitable for most purposes, but contain 5% of phosphine according to ^1H NMR; analytically pure samples can be obtained by recrystallisation from a hexane/CH_2Cl_2 mixture at −30 °C. Samples suitable for X-ray diffraction studies can be obtained by slow evaporation from a pentane solution. IR (CH_2Cl_2): $\nu_{CO} = 1961\ cm^{-1}$. Anal. Calcd. for $C_{42}H_{58}O_3PRh$: C, 67.73; H, 7.85: Found: C, 67.99; H, 7.47. ^1H NMR (300 MHz, $CDCl_3$, 298 K): δ 7.56 (br, 4 H, *o*-Dtbp), 7.50–7.45 (m, 3 H, *p*-C_6H_3, *p*-Dtbp), 7.30 (dd, $^3J_{HH} = 7.4$ Hz, $^4J_{HP} = 3.0$ Hz, 2 H, *m*-C_6H_3), 5.47 (s, 1 H, *CH* acac), 2.06 (s, 3 H, CH_3 acac), 1.54 (s, 3 H, CH_3 acac), 1.36 (s, 36 H, CH_3 ^{t}Bu), 0.77 (dd, $^2J_{HP} = 9.1$ Hz, $^3J_{HRh} = 1.9$ Hz, 6 H, P–CH_3). $^{13}C\{^1H\}$ NMR (100 MHz, $CDCl_3$, 298 K): δ 189.7 (dd, $^1J_{CRh} = 78$ Hz, $^2J_{CP} = 27$ Hz, *CO*), 187.8 (s, *CO* acac), 184.8 (s, *CO* acac), 151.0 (s, *m*-Dtbp), 147.9 (d, $^2J_{CP} = 7$ Hz, *o*-C_6H_3), 142.5 (d, $^3J_{CP} = 3$ Hz, *ipso*-Dtbp), 130.7 (d, $^1J_{CP} = 41$ Hz, *ipso*-C_6H_3), 130.5 (d, $^3J_{CP} = 7$ Hz, *m*-C_6H_3), 128.6 (d, $^4J_{CP} = 2$ Hz, *p*-C_6H_3), 124.7 (s, *m*-Dtbp), 121.7 (s, *p*-Dtbp), 100.5 (d, $^4J_{CP} = 2$ Hz, *CH* acac), 35.1 (s, C ^{t}Bu), 31.7 (s, CH_3 ^{t}Bu), 27.8 (d, $^4J_{CP} = 5$ Hz, CH_3 acac), 27.3 (s, CH_3 acac), 20.4 (dd, $^1J_{CP} = 38$ Hz, $^3J_{CRh} = 2$ Hz, P–CH_3). $^{31}P\{^1H\}$ NMR (162 MHz, CD_2Cl_2, 298 K): δ 28.4 (d, $^1J_{PRh} = 167$ Hz).

4. Conclusions

We have evaluated the stereoelectronic properties of 12 sterically demanding dialkylterphenyl phosphines, PR_2Ar', employing various approaches. The ligands analyzed herein have permitted interrogating the effects of using methyl or larger branched and cyclic R groups at the phosphorus center (series **L1-L5** and **L6-L9**) and those derived from increasing the size of distant substituents (series **L9-L12**) or modifying their positions (**L1** vs. **L9-L12**) at the terphenyl fragment.

Tolman Electronic Parameters (TEP) have been calculated from infrared data on CO stretching frequencies of $IrCl(CO)_2(PR_2Ar')$ and $Rh(acac)(CO)_2(PR_2Ar')$ complexes. Although a fair correlation was found for ν_{CO} data derived from iridium and rhodium complexes, those results differ somewhat from the ones obtained from $Ni(CO)_3(PR_2Ar')$ species. This difference could be attributed to the different nature of the complexes utilized for the parameterization. On the other hand, $^{31}P–^{77}Se$ scalar coupling constants correlate better with TEP(Ni) parameters, although the method fails when series of ligands that create very different front-strain are confronted. On this basis, we conclude that the selection of a single method to grade ligand σ-donor capacity should be handled with caution, and advise employing a combination of the different available parameters to obtain truly reliable information.

The steric properties of terphenyl phosphines have also been examined by means of Tolman Cone Angles (TCAs), ligand shielding (G) and percent buried volume (%VBur) calculations from experimental X-ray diffraction data and DFT-optimized geometries. These results point out that: (i) the steric protection provided by terphenyl phosphines as monodentated κ[1]-P ligands is considerably superior to that conferred by the widely employed biaryl counterparts; (ii) substituting the methyl groups in PMe_2Ar' by other hydrocarbyl fragments has the most prominent effect on all calculated steric descriptors; (iii) in $IrCl(CO)_2(PR_2Ar')$ complexes, terphenyl phosphines seem to exert their steric demands in closer proximity to the metal center than their PCy_2(biaryl) counterparts.

Acknowledgements

We thank MICIU (Grants CTQ2013-42501-P, CTQ2016-75193P, CTQ2014-52769-C3-3-Rand CTQ2017-82893-C2-2-R) for financial support. J.J .M., M. M. G. and M. M. A. thank the Universidad de Sevilla (V Plan Propio de Investigación) and MICIU for research fellowships. The Supercomputing Centre of Galicia (CESGA); Centro de Servicios de Informática y Redes de Comunicaciones (CSIRC) of the Universidad de Granada are acknowledged for providing the computing time.

Appendix A. Supplementary data

Supplementary data to this article can be found online at https://doi.org/10.1016/j.jorganchem.2019.06.003.

References

[1] See for example: (a) M. Huser, M.-T. Youinou, J.A. Osborn, Angew Chem. Int. Ed. Engl. 28 (1989) 1386;
(b) Y. Ben-David, M. Portnoy, D. Milstein, J. Am. Chem. Soc. 111 (1989) 8742;
(c) A.F. Littke, G.C. Fu, Angew. Chem. Int. Ed. 37 (1998) 3387;
(d) H. Doucet, T. Ohkuma, K. Murata, T. Yokozawa, M. Kozawa, E. Katayama, A.F. England, T. Ikariya, R. Noyori, Angew. Chem. Int. Ed. 37 (1998) 1703;
(e) M.S. Sanford, J.A. Love, R.H. Grubbs, J. Am. Chem. Soc. 123 (2001) 6543;
(f) T.E. Barder, S.D. Walker, J.R. Martinelli, S.L. Buchwald, J. Am. Chem. Soc. 127 (2005) 4685;
(g) L. Chen, P. Ren, B.P. Carrow, J. Am. Chem. Soc. 138 (2016) 6392.
[2] (a) M. Bochmann, Organometallic and Catalysis. An Introduction, Oxford University Press, Oxford, 2015;
(b) J.F. Hartwig, Organotransition Metal Chemistry, From Bonding to Catalysis, Sausalito, 2010;
(c) D.H. Valentine, J.H. Hillhouse, Synthesis (2003) 2437.
[3] C.A. Tolman, Chem. Rev. 77 (1977) 313.
[4] (a) T.J. Colacot (Ed.), New Trends in Cross Coupling. Theory and Applications, RSC Publishing, Cambridge, UK, 2015, pp. 20–90;
(b) C.A. Fleckenstein, H. Plenio, Chem. Soc. Rev. 39 (2010) 694.
[5] A.F. Littke, G.C. Fu, Angew. Chem. Int. Ed. 41 (2002) 4176.
[6] A.J. Kendall, D.R. Tyler, Dalton Trans. 44 (2015) 12473.
[7] (a) A. Zapf, A. Ehrentraut, Angew. Chem. Int. Ed. 39 (2000) 4153.
[8] (a) J.F. Hartwig, M. Kawatsura, S.I. Hauck, K.H. Shaughnessy, L.M. Alcazar-Roman, J. Org. Chem. 64 (1999) 5575;
(b) G. Mann, C. Incarvito, A.L. Rheingold, J.F. Hartwig, J. Am. Chem. Soc. 121 (1999) 3224;
(c) Q. Shelby, N. Kataoka, G. Mann, J. Hartwig, J. Am. Chem. Soc. 122 (2000) 10718.
[9] (a) J.P. Wolfe, R.A. Singer, B.H. Yang, S.L. Buchwald, J. Am. Chem. Soc. 121 (1999) 9550;
(b) R. Martin, S.L. Buchwald, Acc. Chem. Res. 41 (2008) 1461;
(c) D.S. Surry, S.L. Buchwald, Angew. Chem. Int. Ed. 47 (2008) 6338.
[10] N. Hoshiya, S.L. Buchwald, Adv. Synth. Catal. 354 (2012) 2031.
[11] See for example: (a) P. Ruiz-Castillo, S.L. Buchwald, Chem. Rev. 116 (2016) 12564;
(b) D. Maitis, B.P. Fors, J.L. Henderson, Y. Nakamura, S.L. Buchwald, Chem. Sci. 2 (2011) 57;
(c) M.A. Düfert, K.L. Billingsley, S.L. Buchwald, J. Am. Chem. Soc. 135 (2013)

1287;
(d) C.W. Cheung, S.L. Buchwald, Org. Lett. 15 (2013) 3998;
(e) X. Wu, B.P. Fors, S.L. Buchwald, Angew. Chem. Int. Ed. 50 (2011) 9943.
[12] (a) T. Nguyen, A.D. Sutton, M. Brynda, J.C. Fettinger, G.J. Long, P.P. Power, Science 310 (2005) 844;
(b) M. Carrasco, M. Faust, R. Peloso, A. Rodríguez, J. López-Serrano, E. Álvarez, C. Maya, P.P. Power, E. Carmona, Chem. Commun. 48 (2015) 3954;
(c) M. Carrasco, I. Mendoza, M. Faust, J. López-Serrano, R. Peloso, A. Rodríguez, E. Álvarez, C. Maya, P.P. Power, E. Carmona, J. Am. Chem. Soc. 136 (2014) 9173;
(d) M. Carrasco, I. Mendoza, E. Álvarez, A. Grirrane, C. Maya, R. Peloso, A. Rodríguez, A. Falceto, S. Álvarez, E. Carmona, Chem. Eur J. 21 (2015) 410.
[13] (a) R.C. Smith, R.A. Woloszynek, W. Chen, T. Ren, J.D. Protasiewicz, Tetrahedron Lett. 45 (2004) 8327;
(b) B. Buster, A.A. Diaz, T. Graham, R. Khan, M.A. Khan, D.R. Powell, R.J. Wehmschulte, Inorg. Chim. Acta 362 (2009) 3465;
(c) S. Sasaki, R. Chowdhury, M. Yoshifuji, Tetrahedron Lett. 45 (2004) 9193;
(d) S. Sasaki, M. Izawa, M. Yoshifuji, Phosphorus, Sulfur Silicon Relat. Elem. 189 (2014) 1207;
(e) T. Fujihara, K. Semba, J. Terao, Y. Tsuji, Angew. Chem. Int. Ed. 49 (2010) 1472.
[14] (a) J. Campos, L. Ortega-Moreno, S. Conejero, R. Peloso, J. López-Serrano, C. Maya, E. Carmona, Chem. Eur J. 21 (2015) 8883;
(b) M.F. Espada, J. Campos, J. López-Serrano, M.L. Poveda, Angew. Chem. Int. Ed. 54 (2015) 15379;
(c) L. Ortega-Moreno, M. Fernández-Espada, J.J. Moreno, C. Navarro-Gilabert, J. Campos, S. Conejero, J. López-Serrano, C. Maya, R. Peloso, E. Carmona, Polyhedron 116 (2016) 170;
(d) J.J. Moreno, M.F. Espada, E. Krüger, J. López-Serrano, J. Campos, E. Carmona, Eur. J. Inorg. Chem. (2018) 2309;
(e) J.J. Moreno, M.F. Espada, J. Campos, J. López-Serrano, S.A. Macgregor, E. Carmona, J. Am. Chem. Soc. 141 (2019) 2205;
(f) L. Ortega-Moreno, R. Peloso, J. López-Serrano, J. Iglesias-Sigüenza, C. Maya, E. Carmona, Angew. Chem. Int. Ed. 129 (2017) 2816.
[15] M. Marín, J.J. Moreno, C. Navarro-Gilabert, E. Álvarez, C. Maya, R. Peloso, M.C. Nicasio, E. Carmona, Chem. Eur J. 25 (2019) 260.
[16] (a) C.A. Tolman, J. Am. Chem. Soc. 92 (1970) 2953;
(b) C.A. Tolman, J. Am. Chem. Soc. 92 (1970) 2956.
[17] (a) R. Dorta, E.D. Stevens, C.D. Hoff, S.P. Nolan, J. Am. Chem. Soc. 125 (2003) 10490;
(b) R. Dorta, E.D. Stevens, N.M. Scott, C. Costabile, L. Cavallo, C.D. Hoff, S.P. Nolan, J. Am. Chem. Soc. 127 (2005) 2485;
(c) O. Diebolt, G.C. Fortman, H. Clavier, A.M.Z. Slawin, E.C. Escudero-Adán, J. Benet-Buchholz, S.P. Nolan, Organometallics 30 (2011) 1668.
[18] (a) A.R. Chianese, X. Li, M.C. Janzen, J.W. Faller, R.H. Crabtree, Organometallics 22 (2003) 1663;
(b) R.A. Kely III, H. Clavier, S. Giudice, N.M. Scott, E.D. Stevens, J. Bordner, I. Samardjiev, C.D. Hoff, L. Cavallo, S.P. Nolan, Organometallics 27 (2008) 202.
[19] W.J. Stec, A. Okruszek, B. Uznanski, J. Michalski, Phosphorus 2 (1972) 97.
[20] (a) O. Back, M. Henry-Ellinger, C.D. Martin, D. Martin, G. Bertrand, Angew. Chem. Int. Ed. 52 (2013) 2939;
(b) A. Liske, K. Verlinden, H. Buhl, K. Schaper, C. Ganter, Organometallics 32 (2013) 5269;
(c) S.V.C. Vummaleti, D.J. Nelson, A. Poater, A. Gómez-Suárez, D.B. Cordes, A.M.Z. Slawin, S.P. Nolan, L. Cavallo, Chem. Sci. 6 (2015) 1895.
[21] S. Álvarez, Dalton Trans. 42 (2013) 8617.
[22] (a) D.L. Liptrot, D.P. Power, Nat. Chem. Rev. 1 (2017) 0004.
(b) J.P. Wagner, P.R. Schreiner, Angew. Chem. Int. Ed. 54 (2015) 12274.
(c) J.-D. Guo, D.J. Liptrot, S. Nagase, P.P. Power, Chem. Sci. 6 (2015) 6235.
[23] B.J. Dunne, R.B. Morris, A.G. Orpen, J. Chem. Soc., Dalton Trans. (1991) 653.
[24] (a) P.A.W. Dean, Can. J. Chem. 57 (1979) 754;
(b) A. Cogne, A. Grand, J. Laugier, J.B. Robert, L. Wiesenfeld, J. Am. Chem. Soc. 102 (1980) 2238;
(c) S.W. Carr, R. Colton, Aust. J. Chem. 34 (1981) 35;
(d) A. Tohmé, H. Sahnoune, T. Roisnel, V. Dorcet, J.-F. Halet, F. Paul, Organometallics 33 (2014) 3385.
[25] J. Autschbach, B. Le Guennic, J Chem. Educ. (2007) 156.
[26] (a) H.A. Bent, Chem. Rev. 61 (1961) 275;
(b) W. McFarlane, D.S. Rycroft, J. Chem. Soc., Dalton Trans. (1973) 2162;
(c) I.V. Alabugin, S. Bresch, G.D.P. Gomes, J. Phys. Org. Chem. 28 (2015) 147.
[27] U. Beckmann, D. Süslüyan, P.C. Kunz, Phosphorus, Sulfur Silicon Relat. Elem. 186 (2011) 2061.
[28] (a) R.P. Pinnell, C.A. Megerle, S.L. Manatt, P.A. Kroon, J. Am. Chem. Soc. 95 (1973) 977;
(b) R.D. Kroshefsky, R. Weiss, J.G. Verkade, Inorg. Chem. 18 (1979) 469.
[29] T.E. Müller, D.M.P. Mingos, Transit. Met. Chem. 20 (1995) 533.
[30] See for example: (a) A. Grirrane, H. García, A. Corma, E. Álvarez, Chem. Eur J. 19 (2013) 12239;
(b) P. Pérez-Galán, N. Delpont, E. Herrero-Gémez, F. Maseras, A.M. Echavarren, Chem. Eur. J. 16 (2010) 5324.
[31] I.A. Guzei, M. Wendta, Dalton Trans (2006) 3991.
[32] (a) A. Poater, F. Ragone, S. Giudice, C. Costabile, R. Dorta, S.P. Nolan, L. Cavallo, L., Organometallics 27 (2008) 2679;
(b) A. Poater, B. Cosenza, A. Correa, S. Giudice, F. Ragone, V. Scarano, L. Cavallo, Eur. J. Inorg. Chem. (2009) 1759.
[33] (a) K. Wu, A.G. Doyle, Nat. Chem. 9 (2017) 779;
(b) D.J. Durand, N. Fey, Chem. Rev. (2019), https://doi.org/10.1021/acs.chemrev.8b00588.
[34] A. Guzei, M. Wendta, Dalton Trans. (2006) 3991. http://xray.chem.wisc.edu/Resources.html.
[35] Z.L. Niemeyer, A. Milo, D.P. Hickey, M.S. Sigman, Nat. Chem. 8 (2016) 610.
[36] M.H. Keylor, Z.L. Niemeyer, M.S. Sigman, K.L. Tan, J. Am. Chem. Soc. 139 (2017) 10613.
[37] O. Diebolt, G.C. Fortman, H. Clavier, A.M.Z. Slawin, E.C. Escudero-Adan, J. Benet-Buchholz, S.P. Nolan, Organometallics 30 (2011) 1668.
[38] As Expected, There Is a Linear Correlation, R = 0.84, between the $\%V_{Bur}$ and Equivalent Cone Angle (ECA) when Combined Experimental Data from Therphenyl and Biarylphosphines Is Use, Suggesting that ECA Do Not Capture Distant Steric Effects like the Tolman Cone Angle; see the supporting information for details.
[39] (a) B. Schiemenz, P.P. Power, Organometallics 15 (1996) 958;
(b) R.S. Simons, S.T. Haubrich, B.V. Mork, M. Niemeyer, P.P. Power, Main Group Chem. 2 (1998) 275.
[40] J.W. Wielandt, D. Ruckerbauer, Inorg. Synth. 35 (2010) 120.
[41] J.L. Herde, J.C. Lambert, C.V. Senoff, M.A. Cushing, Inorg. Synth. 15 (2007) 18.